Sensors & Actuators: B. Chemical 283 (2019) 890–896

Contents lists available at ScienceDirect

Sensors and Actuators B: Chemical

journal homepage: www.elsevier.com/locate/snb

Enhanced hydrogen sensing properties of Pd-coated SnO_2 nanorod arrays in nitrogen and transformer oil

Min Hyung Kim[a], Byungjin Jang[a], Wonkyung Kim[b], Wooyoung Lee[a,*]

[a] Department of Materials Science and Engineering, Yonsei University, 262 Seongsanno, Seodaemun-gu, Seoul, 129-749, Republic of Korea
[b] School of Nano & Materials Science and Engineering, Kyungpook National University, 2559Gyeongsang-daero, Gyeongsangbuk-do, 37224, Republic of Korea

ARTICLE INFO

Keywords:
Hydrogen sensing
SnO2
Pd
Nanorod arrays
Transformer oil

ABSTRACT

We report enhanced sensing properties of Pd-coated SnO_2 nanorod (NR) arrays for detecting H_2 gas in N_2 and dissolved in transformer oil. The Pd nanoparticles were coated on randomly ordered vertical SnO_2 NR arrays by the glancing angle deposition (GLAD) method, which utilizes an electron-beam evaporator and a DC magnetron sputtering system. The Pd-coated SnO_2 NR arrays exhibited high response (104 at 1% H_2) in N_2. Pd-coated SnO_2 NR arrays were immersed and in mineral oil that contains various concentrations of dissolved H_2 and the electrical response was measured. We found that the Pd-coated SnO_2 NR arrays showed superior response (R = ~96), low detection limit (0.3 ppm), and fast response times (300 s). The Pd-coated SnO_2 NR arrays had a temperature coefficient of resistance (TCR) of 3.69 × 10-3 $°C^{-1}$ at various oil temperatures (20–80 °C), indicating good thermal stability at high temperatures. The sensing mechanism of the Pd-coated SnO_2 NR arrays was also demonstrated by using changes in the Schottky barrier height at the Pd/SnO_2 interface upon exposure to H_2.

1. Introduction

Analyzing gases dissolved in insulating oil for monitoring failure of the internal components of power transformers is one of the most pressing issues in the electric power industry. Deterioration of mineral oil and insulating paper in a transformer occurs under abnormal conditions, making dielectric insulation impossible [1–5]. The deterioration causes C–H and C—C bonds in the insulating system to break, thus generating various gases such as H_2, CH_4, C_2H_6, C_2H_2, CO, and CO_2 [1–5]. Among these gases, H_2 is the most important to be monitored since it is generated during both discharge and thermal deterioration of insulating oil and paper. Its concentration is also the highest among 10 kinds of dissolved gases [1–5].

The severity of faults and type of failure can be determined by measuring the concentration of dissolved gases [6]. Transformer abnormality is diagnosed using dissolved gas analysis (DGA) [6]. Until recently, as a kind of the off-line measurement, gas chromatography has been used to analyze the oil gathered from the transformer [7–9]. This method consumes time and manpower, requires expensive equipment, and has a measurement error caused by the lack of real-time monitoring [7–9]. Due to these issues, optical [10–12], diode [13,14] and resistive [15–17] immersed gas sensors have been developed that can continuously monitor dissolved gases in-situ. In recent years, we have reported the H_2 gas sensing properties of Pd-coated *p*-type Si nanowire (NW) arrays for detection of dissolved H_2 in oil [18]. The Pd-coated Si NW arrays exhibit prominent sensing performance at room temperature (20 °C) in terms of response (~10), response time (600 s), and low detection limit (1 ppm) [18]. However, we found that there is a decrease in response at elevated temperatures in oil (R = 2.2 at 70 °C, 460 ppm H_2). A solution to work out the stability problem at elevated temperatures is necessary.

Here, we report the H_2 sensing properties of Pd-coated SnO_2 NR arrays fabricated by glancing angle deposition (GLAD) in N_2 and transformer oil. The length of SnO_2 NRs was controlled to obtain optimal H_2 sensing performance. The real-time response of Pd-coated SnO_2 NR arrays was measured for various H_2 concentrations in both N_2 and transformer oil. The electrical response of Pd-coated SnO_2 NR arrays for specific H_2 concentrations was also measured at various temperatures (20–80 °C). In order to clarify the sensing mechanism, we focused on the Schottky barrier variation upon exposure to H_2 at the Pd-SnO_2 interface. This will be addressed in detail below.

* Corresponding author.
E-mail address: wooyoung@yonsei.ac.kr (W. Lee).

https://doi.org/10.1016/j.snb.2018.12.063
Received 20 June 2018; Received in revised form 9 November 2018; Accepted 11 December 2018
Available online 23 December 2018

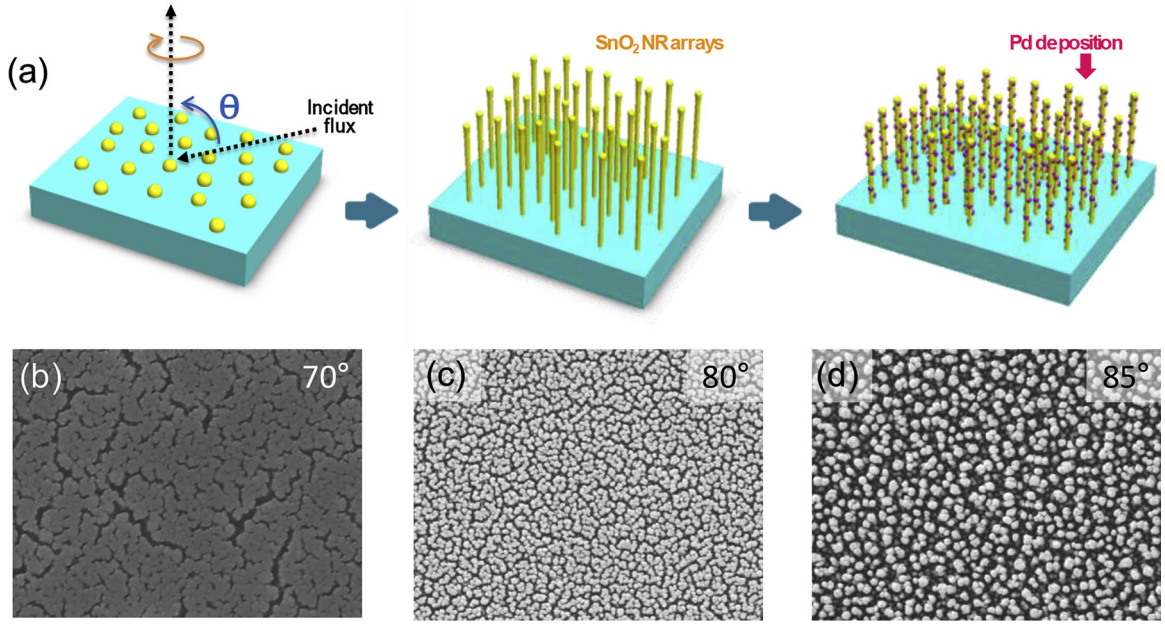

Fig. 1. (a) Schematic illustration of the fabrication process of Pd-coated SnO_2 NR arrays. (b–d) Top-view SEM images of the vertically ordered SnO_2 NR arrays as a function of incident angle (70°, 80°, and 85°).

2. Experiment

2.1. Fabrication of Pd-coated SnO2 NR arrays

Fig. 1(a) shows a schematic of the overall fabrication process of Pd-coated SnO_2 NR arrays. Randomly ordered SnO_2 NR arrays were fabricated by GLAD using an E-beam evaporator [19–21]. 1 × 1 cm^2 SiO_2/Si substrates were diced from a wafer and were sequentially cleaned in acetone, methanol, and deionized water. The cleaned substrates were finally dried with nitrogen (N_2). The cleaned wafers were attached to the holder and tilted to a constant incident angle. Subsequently, ~3 mm SnO_2 grains (4 N purity, Kojundo Chemical Laboratory Co., Ltd) were placed in a 7 cc-crucible and located under the holder. Vertically standing SnO_2 NR arrays were deposited on the 70°, 80°, and 85° tilted substrates rotating at a speed of 15 rpm. Process conditions include an initial pressure of 5.0 × 10^{-6} Torr and a growth rate of 1 Å/s. After deposition, the samples were heat treated at 550 °C for 2 h.

Five-nanometer Pd films were sputtered on the vertically ordered SnO_2 NR arrays through an ultra-high vacuum DC magnetron sputtering system (SNTEK Co., Ltd). When the base pressure reached 4.1 × 10^{-7} torr, 34 sccm of Ar was injected to start deposition. The working pressure at the time of deposition was 2.3 × 10^{-3} torr, and the Pd deposition rate was ~4.7 Å/s at 20 W.

2.2. Characterization and I–V measurements

The morphologies of the Pd-coated SnO_2 NR arrays were characterized using field-emission scanning electron microscopy (FE-SEM; JSM-7100 F, JEOL Ltd.). Pd films deposited on the surface of the SnO_2 NR arrays were examined with an energy dispersive X-ray spectrometer (FE-SEM-EDS; JEOL-7100 F, JEOL Ltd.).

I–V measurements of the Pd-coated SnO_2 NR arrays were conducted by exposing to air, 10 ppm, and 1% H_2 in ambient conditions. After the reaction saturated, the voltage was changed within the -4 to +4 V range and was controlled with a Keithley 236 SMU, and the current in the sensor was measured.

2.3. Sensing measurement

The Pd-coated SnO_2 NR arrays grown onto the SiO_2/Si substrates were loaded onto a printed circuit board (PCB). Line electrodes were constructed parallelly on each top side of the Pd-coated SnO_2 NR arrays, being connected to the PCB by using silver paste (P-100, Cans Inc.) [Baek, Jang]. The constructed electrodes were dried at ambient atmosphere for 4 h. For the H_2 sensing measurement in N_2 atmosphere, the sensor device of the Pd-coated SnO_2 NR arrays loaded onto the PCB is mounted in a home-made gas chamber [22]. The measurement in N_2 atmosphere was performed at room temperature. The real-time resistance was measured by applying a constant voltage (0.1 V) for a time interval of 1 s using the measurement unit (Keithley 236 SMU, Keithley Instruments Inc.). The gas flow rate was fixed at 500 sccm by a mass flow controller (MFC). The Pd-coated SnO_2 NR arrays were tested by varying H_2 concentration from 0.2 to 10,000 ppm in N_2 atmosphere. For the H_2 sensing measurement in oil, the Pd-coated SnO_2 NR array loaded onto the PCB was mounted on a device composed of a polyimide-based plastic outer-shell, which had a 0.8 × 0.8 cm^2 square open window, and the assembly was directly submerged in oil through a cable port [18]. The details of the oil gas-testing equipment were described in our previous paper [18]. The measurement in oil chamber was performed at temperatures in the 20–80 °C range, and temperature was controlled using a heating cable. H_2 was bubbled into the chamber at atmospheric pressure and dissolved in mineral oil (KS 1#2, DONGNAM Petroleum Ind. Co. Ltd.). H_2 measurements in oil were carried out in the same manner as in the N_2 ambient test.

3. Results and discussion

It is well known that the GLAD creates an oblique deposition geometry by tilting the substrate to a glancing angle [21]. The glancing angle (θ) between the surface normal and incident vapor leads to a shadowing effect between vaporizing flux and pre-evaporated SnO_2 nuclei and enables modification of the average NR diameter and density [20,21]. Among the factors that can be used to control the density and perpendicularity of the nanostructures, high deposition angle and fast rotation yields a vertically oriented columnar morphology (see Fig. 1(a)) [21]. The density of the SnO_2 NRs was controlled by selecting the appropriate glancing angle, as shown in Fig. 1(b)–(d). Each shows the top surface morphology of the SnO_2 NR arrays with incident angle of 70°, 80°, and 85°, respectively.

Fig. 2(a)–(c) shows the SEM images of the top, tilted, and cross-

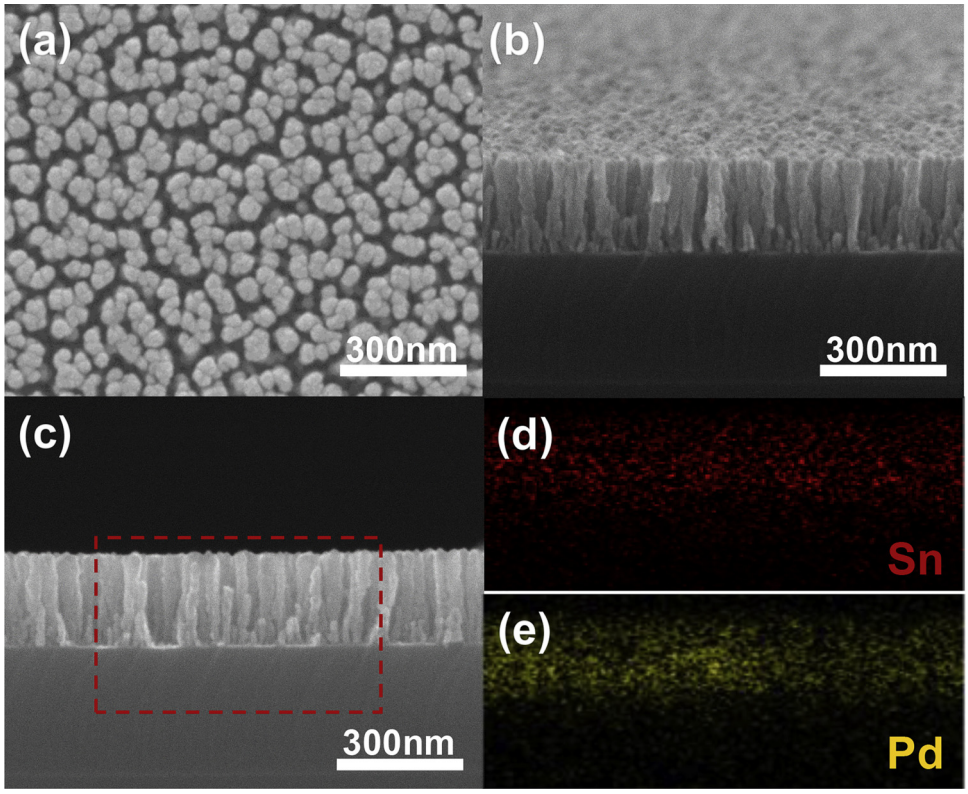

Fig. 2. SEM images of Pd-coated SnO_2 NR arrays. (a) Top view, (b) tilted view, (c) cross-sectional view, and (d–e) EDX mapping of the magnified cross-sectional view.

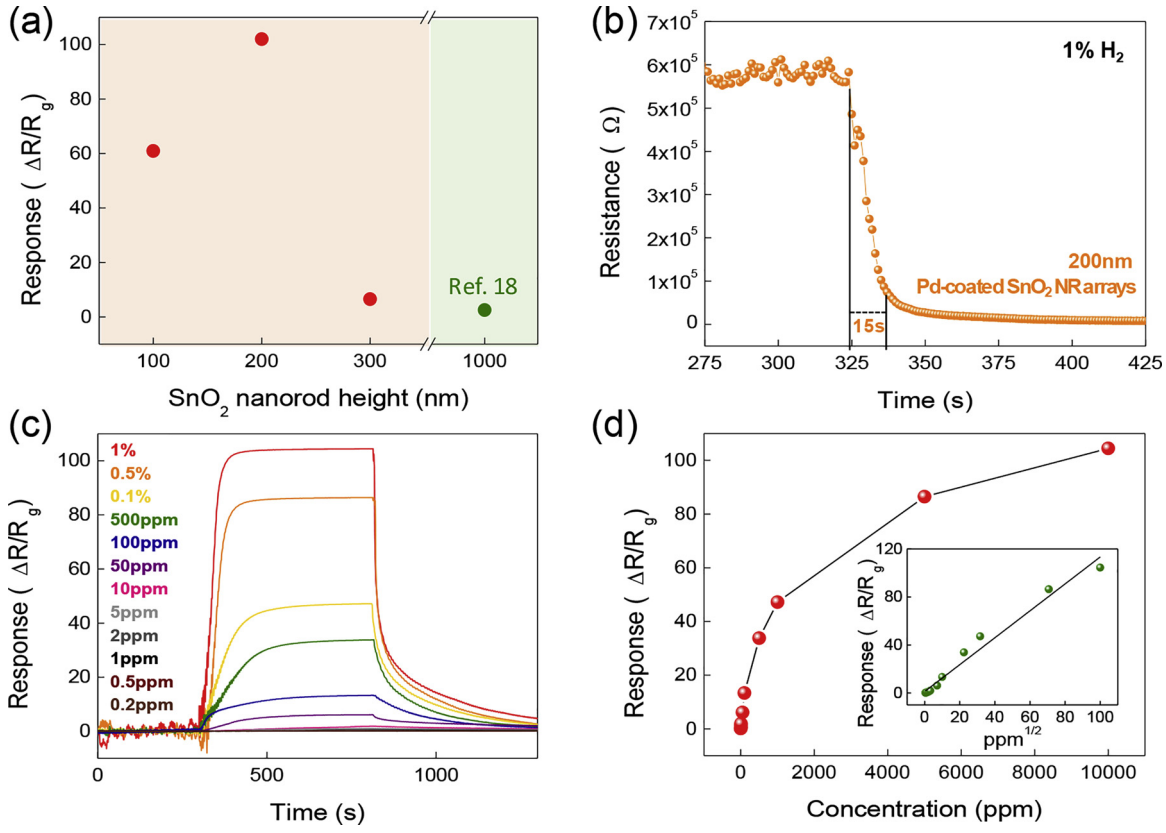

Fig. 3. (a) Response of 100, 200, 300, and 1000 nm long Pd-coated SnO_2 NR arrays to 1% H_2. (b) Resistance variation of Pd-coated SnO_2 NR arrays with optimal thickness of 200 nm at 1% H_2. (c) Response vs. time plot of Pd-coated SnO_2 NR arrays with various H_2 concentrations. Plots of responses as a function of (d) H_2 concentration and (inset) square root of H_2 concentration.

Table 1
Sensing properties of Pd/SnO_2-based H_2 sensors at room temperature operation.

Materials	Response ($\Delta R/R_g$)	Operating temp. (°C)	Lowest Detection Limit (ppm)	Response time (sec)	Ref.
SnO_2-Pd-Au composite	0.02 (1% H_2)	RT	134	60	[25]
Pd-doped SnO_2 nanowires	43.8 (0.1% H_2)	RT	100	138	[26]
Pd/SnO_2 nanoclusters	0.6 (1% H_2)	RT - 80	5000	41	[27]
Nanocrystalline SnO_2 thin films with Pd grid	6.0 (0.1% H_2)	RT - 125	150	205	[28]
Pd/SnO_2/RGO nanocomposites	1.2 (1% H_2)	RT - 45	100	123	[29]
Pd-coated SnO_2 NR arrays	104 (1% H_2)	RT	0.2	15	This work

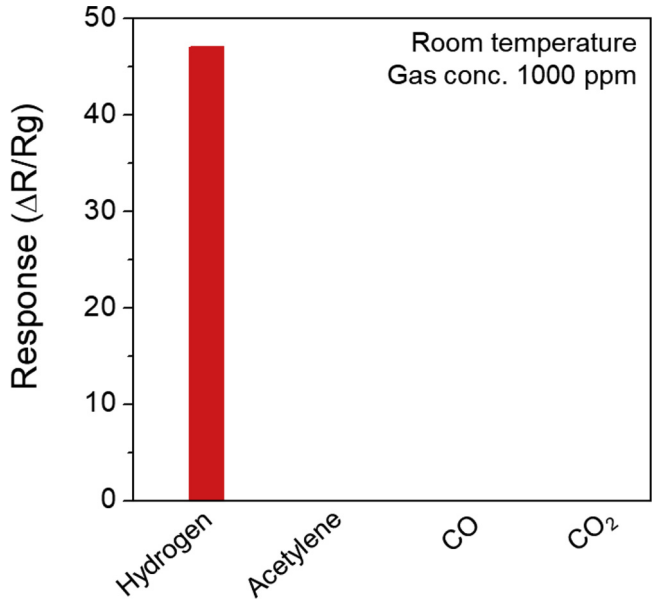

Fig. 4. Sensing response of Pd-coated SnO_2 NR arrays to 1000 ppm of H_2 and other common transformer oil gases (acetylene, CO, and CO_2) at room temperature.

sectional views of the Pd-coated SnO_2 NR arrays, respectively. The optimal fabrication conditions were obtained by controlling the SnO_2 NR growth via employing different deposition times and glancing angles. As shown in the SEM image in Fig. 2(a)–(c), vertically standing NRs were randomly spaced with an average diameter of ~30 nm, an average height of 200 nm, and an average spacing of 20–40 nm. Energy dispersive X-ray (EDX) mapping of the magnified cross-sectional SEM image is shown in Fig. 2(d) and Fig. 2(e). Pd nanoparticles were deposited on the overall surfaces of the SnO_2 NR arrays, facilitating the formation of a Schottky contact at the interface between Pd nanoparticles and SnO_2 NRs.

The H_2 sensing performance of the Pd-coated SnO_2 NR arrays in N_2 is shown in Fig. 3. Specifically, the responses of Pd-coated SnO_2 NR arrays were measured as a function of the height of the SnO_2 NRs (see Fig. 3(a)). The response is defined as $R = (R_0\text{-}R_g)/R_g$, where R_0 and R_g indicate the electrical resistances before and after H_2 exposure, respectively. As shown in Fig. 3(a), 200 nm-tall Pd-coated SnO_2 NR arrays showed highly enhanced H_2 response (R = 104 at 1% H_2), which was higher than that of 1000 nm SnO_2 NRs (R = 2.3 at 1% H_2) by a factor of 45 [19]. Fig. 3(b) shows a resistance curve of the Pd-coated SnO_2 NR arrays with optimal thickness of 200 nm upon exposure to 1% H_2. When exposed to H_2, the resistance of the Pd-coated SnO_2 NR arrays decreased from the base resistance value. The response time of the Pd-coated SnO_2 NR arrays was defined as the time required to reach 90% of the total change in resistance. This was found to be 15 s for 1% H_2. The real-time response of 200 nm Pd-coated SnO_2 NR arrays was measured with various H_2 concentrations (10,000–0.2 ppm) in N_2 at room temperature, as shown in Fig. 3(c). The maximum response value was 104 for 1% H_2. The response plots show a parabolic curvature for specific H_2 concentrations, as shown in Fig. 3(d). The response for specific H_2 concentrations were plotted as a function of the square root of H_2 concentration (see the inset in Fig. 3(d)), showing a linear dependence of changes in response to H_2 concentration (correlation constant, r = 0.98), in accordance with Sievert's Law [23,24]. Compared to other Pd/SnO_2 based room-temperature H_2 sensors reported in the literature, Pd-coated SnO_2 NR arrays show superior sensing performance in N_2 in terms of high response, low detection limit, and fast response time (see Table. 1). Moreover, Fig. 4 exhibits the sensing response of Pd-coated

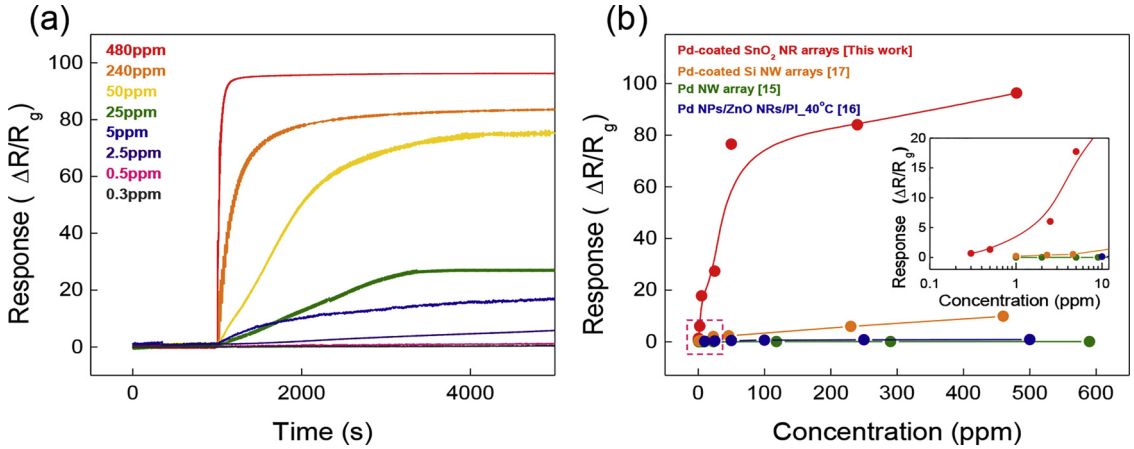

Fig. 5. (a) Real-time response curves for SnO_2 NR arrays for various H_2 concentrations in oil. (b) Responses of resistive H_2 sensors for detection of H_2 in transformer oil.

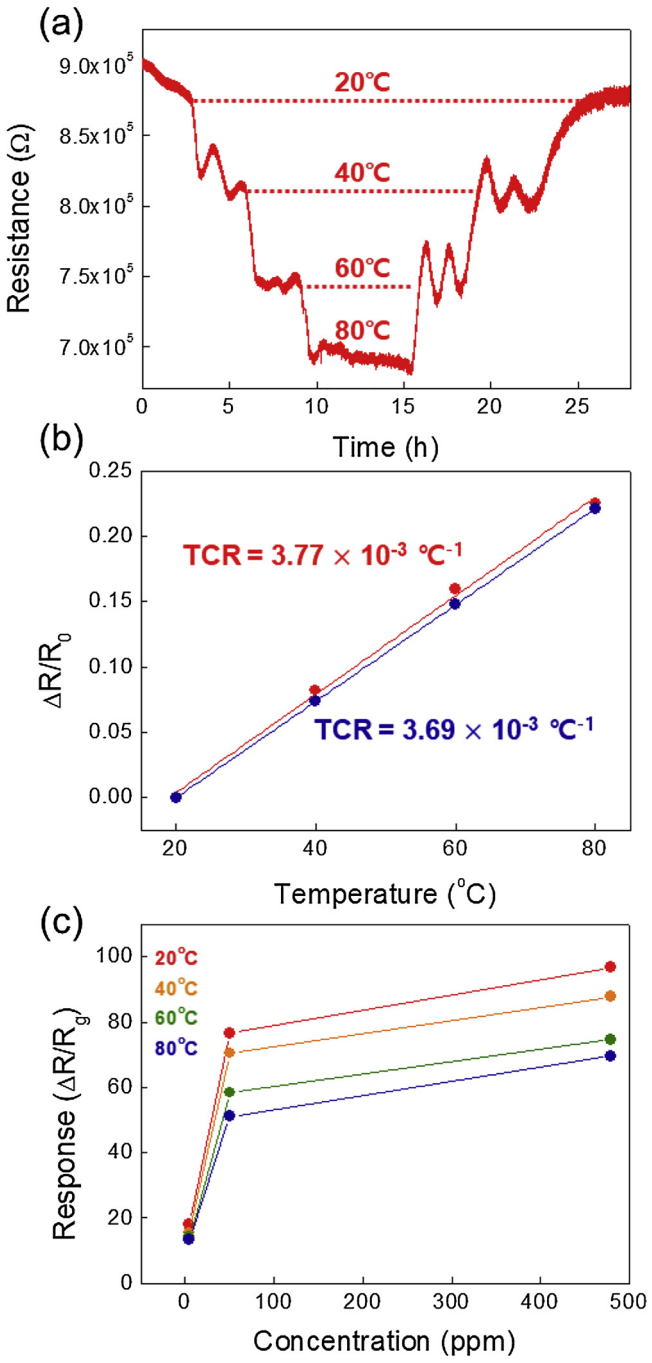

Fig. 6. Temperature dependence of Pd-coated SnO_2 NR arrays at temperature in the 20–80 °C range in oil. (a) Plot of resistance variation depending on stepwise temperature modulation. (b) Replot of the resistance change ratio vs. temperature. (c) Response curves as a function of H_2 concentration in oil at various temperatures (20–80 °C).

SnO_2 NR arrays towards 1000 ppm of H_2 and other common transformer oil gases (C_2H_2, CO, and CO_2) at room temperature. The Pd-coated SnO_2 NR arrays only response to H_2, indicating that the Pd-coated SnO_2 NR arrays shows good selective for H_2 compared to C_2H_2, CO, and CO_2. This is due to the excellent catalytic effect of Pd on H_2 even at the low temperature.

The Ostwald coefficient is a concept derived from Henry's law, which states that the concentration of dissolved gas in liquid is proportional to the partial pressure in the gas phase [30]. This indicates the solubility of a gas per unit volume at a specific temperature and pressure. The solubility of H_2 in the oil was calculated in accordance with the Ostwald coefficient [31]. The Ostwald coefficient is defined as:

$$L_c = 2.31exp\left[\left(\frac{0.639(700-T)}{T}\right)ln(3.333L_0)\right](0.980-d) \quad (1)$$

where L_c is the Ostwald coefficient at T for a liquid of specified density, T is the specified temperature, d is the density of the liquid at 288 K, and L_0 is the Ostwald coefficient at 273 K for a liquid. According to standard test method for estimation of solubility of gases in petroleum liquids (ASTM D2779), L_0 for H_2 is 0.04, and the density of the oil used in this study is 0.8560 kg/L. Using this equation, we calculated L_c = 480 ppm/% at 20 °C and L_c = 808 ppm/% at 80 °C [31]. In order to measure the concentration of dissolved H_2 in oil, GC analysis (Agilent 7890 A Gas Chromatography, Agilent Technologies) was assisted by Hyundai Electric. The GC analysis was conducted according to Method C of ASTM D 3612, a headspace sampling method [32]. It was found that 475 ppm H_2 was dissolved in the oil when 1% H_2 was blown into the oil-filled chamber at room-temperature (20 °C). This is comparable to the calculated value above (480 ppm/% at 20 °C).

The real-time response of the Pd-coated SnO_2 NR arrays was measured with dissolved H_2 in oil at 20 °C, which ranged from 480 ppm to 0.3 ppm (see Fig. 5(a)). The resistance of the Pd-coated SnO_2 NR arrays decreased rapidly as H_2 was blown into the oil and it eventually became saturated with H_2. At 480 ppm, the maximum response was found to be 96 and the fastest response time was 300 s. The changes in response were plotted as a function of H_2 concentration (see Fig. 5(b)) using the data from Fig. 4(a). Pd-coated SnO_2 NR arrays show excellent performance in terms of response and limit of detection (see Fig. 5(b) inset) compared to other oil-immersed H_2 sensors [16–18].

Fig. 6 shows the temperature dependence of the Pd-coated SnO_2 NR arrays in oil ranging from 20 °C to 80 °C. Fig. 6(a) shows a plot of resistance variation as the temperature changes stepwise. The temperature of the oil was increased with a 20 °C increments and was maintained at each temperature for 2 h. The resistance of the Pd-coated SnO_2 NR arrays decreased at each increment, with the magnitude also depending on increasing temperature. Similarly, resistance incrementally increased with decreasing temperature. Fig. 6(b) shows a replot of the resistance change ratio versus temperature converted from Fig. 6(a) to obtain the temperature coefficient of resistance (TCR, α). The TCR is defined as Eq. (2):

$$TCR(\alpha) = \frac{1}{\Delta T}\frac{R(T)-R(T_0)}{R(T_0)} \quad (2)$$

where ΔT represents the difference between T and T_0. The TCR value of the Pd-coated SnO_2 NR arrays is 3.77×10^{-3} °C^{-1} with increasing temperature and 3.69×10^{-3} °C^{-1} for decreasing temperature. The obtained value is similar to the TCR value for a 200–300 nm SnO_2 thin film ($\alpha \approx 4 \times 10^{-3}$ °C^{-1}) [33]. Fig. 6(c) shows the response of the Pd-coated SnO_2 NR arrays under exposure to various H_2 concentrations in oil at temperatures in the range of 20–80 °C. We found that the H_2 response of Pd-coated SnO_2 NR arrays decreases with increasing oil temperature at specific H_2 concentration values. This may be due to the reduced solubility of H in PdH_x at high temperatures [16,24]. Despite the decreased H_2 response, the Pd-coated SnO_2 NR arrays only 28% variation when exposed to 480 ppm H_2 at 80 °C compared to the response variation (79%) of Pd-coated Si NW arrays exposed to 460 ppm H_2 at 70 °C [18].

The sensing mechanism of the Pd-coated SnO_2 NR arrays can be explained by using a model for general n-type metal oxide based gas sensors, as shown in Fig. 7. When Pd-coated SnO_2 NR arrays are exposed to air, oxygen molecules are adsorbed onto the surface of the Pd-coated SnO_2 NR arrays (Eq. (3)). The adsorbed oxygen molecules capture electrons from the conduction band of the SnO_2 NRs to form O_2^- ions (Eq. (4)) [34]. Pd serves as a catalyst to induce a spillover of dissociating oxygen molecules into atoms and creating O^- ions (Eq. (5)) [35]. This leads to formation of an electron depletion layer on the

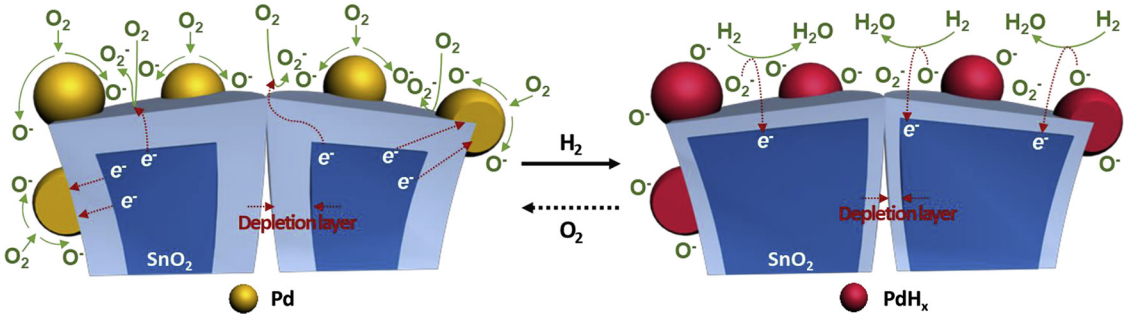

Fig. 7. Schematic images of the sensing reaction mechanism in the Pd-coated SnO_2 NR arrays in air and H_2.

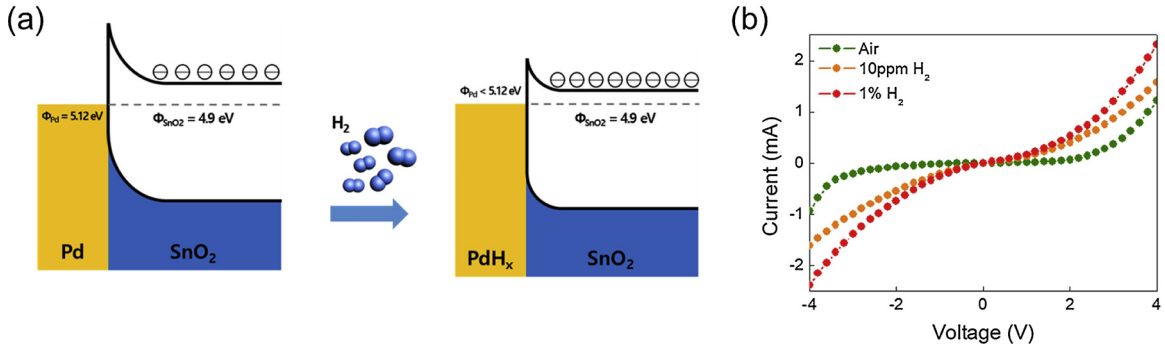

Fig. 8. (a) Schematic illustration of the contact resistance change at the Pd-SnO_2 junction due change in the Schottky barrier ($\phi_M > \phi_S$) before and after exposure to H_2. (b) I–V characteristics for bias voltage ranging from -4 to +4 V, revealing different Schottky barrier height for various H_2 concentrations.

surface of the Pd-coated SnO_2, which increases the resistance of the Pd-coated SnO_2 NR arrays [34,35].

$$O_2(gas) \rightarrow O_2(ads) or\ 2O(ads) \quad (3)$$

$$O_2(ads) + e^- \rightarrow O_2^- \quad (4)$$

$$O(ads) + e^- \rightarrow O^- \quad (5)$$

When exposed to H_2 gas, H_2 molecules decompose into hydrogen atoms (Eq. (6)) and react with the O_2^- or O^- ions (Eqs. (7), (8)) [31,32]. The trapped electrons are then released to the conduction band in the SnO_2 NRs, leading to a decreased resistance in the Pd-coated SnO_2 NR arrays [34,35].

$$H_2(gas) \rightarrow 2H(ads) \quad (6)$$

$$4H(ads) + O_2^-(ads) \rightarrow 2H_2O + e^- \quad (7)$$

$$2H(ads) + O^-(ads) \rightarrow H_2O + e^- \quad (8)$$

The sensing mechanism can be explained in detail by the change in Schottky barrier height at the Pd/SnO_2 interface, as depicted in Fig. 8(a). In the initial state, a Schottky barrier ($\phi_M > \phi_{SC}$) is formed due to the larger work function of Pd (ϕ_{Pd} = 5.12 eV) compared to the work function of SnO_2 (ϕ_{SnO2} = 4.9 eV) [36,37]. After H_2 exposure, dissociated hydrogen atoms convert Pd into PdH_x, thus reducing the work function of Pd ($\phi_{Pd} > \phi_{PdHx}$) and causing the Schottky barrier height to decrease [36,37]. In order to validate the sensing mechanism, Schottky barrier height changes at the interface between Pd and SnO_2 were investigated by measuring the I–V curve upon exposure to H_2. According to the thermionic emission theory, the current through the Schottky contact is inversely proportional to the height of the Schottky barrier [36]. As shown in Fig. 8(b), nonlinear I–V characteristics are observed regardless of H_2 exposure, showing that Schottky contacts are formed in air and in H_2 at ambient conditions. However, the current in the Pd-coated SnO_2 NR arrays shifted with increasing H_2 concentration, indicating a decrease of the Schottky barrier height at the Pd-SnO_2 NR interface when exposed to H_2. This supports the resistance variation in Pd-coated SnO_2 NR arrays explained above.

4. Conclusions

We achieved enhanced H_2 sensing performance of Pd-coated SnO_2 nanorod (NR) arrays for H_2 detection in N_2 and H_2 dissolved in transformer oil. Randomly oriented vertical SnO_2 NR arrays were fabricated using glancing angle deposition (GLAD), and Pd nanoparticles were subsequently sputtered on top of the SnO_2 NRs. Pd-coated SnO_2 NR arrays with 200 nm length were measured at various H_2 concentrations in both N_2 and transformer oil. Excellent H_2 sensing properties were observed in N_2 ambient. In particular, the sensors show high response (˜104), fast response time (15 s), and low detection limit (0.2 ppm) at room temperature. High-performance H_2 sensing properties in oil were obtained with high response of ˜96 and rapid response time (300 s) upon exposure to dissolved H_2 with 480 ppm concentration. The response of the Pd-coated SnO_2 NR arrays to dissolved H_2 in oil was slightly reduced at elevated temperature (28% at 80 °C). Furthermore, the H_2 sensing properties of Pd-coated SnO_2 NR arrays are superior to that of other previously reported oil-immersed-type H_2 sensors. The resistance change of the Pd-coated SnO_2 NR arrays is attributed to changes in the Schottky barrier height at the Pd-SnO_2 NR interface. When exposed to H_2, PdH_x lowers the work function of Pd ($\phi_{Pd} > \phi_{PdHx}$), resulting in a decreased Schottky barrier height. Our results demonstrated that Pd-coated SnO_2 NR arrays show outstanding performance with the potential in degradation monitoring for the internal components of a transformer.

Acknowledgements

This work was supported by the Basic Science Research Program through the National Research Foundation of Korea (NRF), and it was funded by the Ministry of Science, ICT & Future Planning (NFR-2017M3A9F1052297) and the Medium and Large Complex Technology Commercialization Project through the Commercializations Promotion Agency for R&D Outcomes funded by the Ministry of Science and ICT.

References

[1] H.C. Sun, Y.C. Huang, C.M. Huang, A review of dissolved gas analysis in power transformers, Energy Procedia 14 (2012) 1220–1225.
[2] M. Wang, A.J. Vandermaar, K.D. Srivastava, Review of condition assessment of power transformers in service, IEEE Electr. Insul. Mag. 18 (2002) 12–25.
[3] M. Duval, Dissolved gas analysis: it can save your transformer, IEEE Electr. Insul. Mag. 5 (1989) 22–27.
[4] N.A. Muhamad, B.T. Phung, T.R. Blackburn, Dissolved gas analysis for common transformer faults in soy seed-based oil, IET Electr. Power Appl. 5 (2011) 133.
[5] IEC 60599, Mineral Oil-filled Electrical Equipment in Service-guidance on the Interpretation of Dissolved and Free Gases Analysis, Ed. 3.0 (2015), p. 09.
[6] IEEE guide for the interpretation of gases generated in oil-immersed transformers, IEEE Standard C57 (2008) 104.
[7] Y. Leblanc, R. Gilbert, J. Jalbert, M. Duval, J. Hubert, Determination of dissolved gases and furan-related compounds in transformer insulating oils in a single chromatographic run by headspace/ capillary gas chromatography, J. Chromatogr. A 657 (1993) 111–118.
[8] F. Jakob, Dissolved Gas analysis: Past, Present, and Future, (2003).
[9] H. Tsukioka, K. Sugawara, Apparatus for continuously monitoring hydrogen gas dissolved in transformer oil, IEEE Trans. Dielectr. Electr. Insul. E1-16 (1981) 502–509.
[10] N.A. Bakar, A. Abu-Siada, A new method to detect dissolved gases in transformer oil using NIR-IR spectroscopy, IEEE Trans. Dielectr. Electr. Insul. 24 (2017) 409–419.
[11] M. Fisser, R.A. Badcock, P.D. Teal, A. Swanson, A. Hunze, Development of hydrogen sensors based on fiber bragg grating with a palladium foil for online dissolved gas analysis in transformers, Proceedings of SPIE - The International Society for Optical Engineering, (2017), p. 10329.
[12] M.R. Samsudin, Y.G. Shee, F.R. Mahamd Adikan, B.B. Abdul Razak, M. Dahari, Fiber bragg gratings hydrogen sensor for monitoring the degradation of transformer oil, IEEE Sens. J. 16 (2016) 2993–2999.
[13] D. Li, J.W. Medlin, Application of polymer-coated metal-insulator-semicoonductor sensors for the detection of dissolved hydrogen, Appl. Phys. Lett. 88 (2006) 233507.
[14] P. Sandvik, E. Babes-Dornea, A.R. Trudel, M. Georgescu, V. Tilak, D. Renaud, GaN-based schottky diodes for hydrogen sensing in transformer oil, Phys. Stat. Sol. (c) 3 (2006) 2283–2286.
[15] J. Bodzenta, B. Burak, Z. Gacek, W.P. Jakubik, S. Kochowski, M. Urbańczyk, Thin palladium film as a sensor of hydrogen gas dissolved in transformer oil, Sens. Actuators B: Chem. 87 (2002) 82–87.
[16] F. Yang, D. Jung, R.M. Penner, Trace detection of dissolved hydrogen gas in oil using a palladium nanowire array, Anal. Chem. 83 (2011) 9472–9477.
[17] A.S.M. Iftekhar Uddin, U. Yaqoob, G.-S. Chung, Dissolved hydrogen gas analysis in transformer oil using catalyst decorated on ZnO nanorod array, Sens. Actuators B: Chem. 226 (2016) 90–95.
[18] B. Jang, M.H. Kim, J. Baek, W. Lee, Highly sensitive hydrogen sensors: Pd-coated Si nanowire arrays for detection of dissolved hydrogen in oil, in preparation, (2018).
[19] Y.S. Shim, B. Jang, J.M. Suh, M.S. Noh, S. Kim, S.D. Han, Y.G. Song, D.H. Kim, C.Y. Kang, H.W. Jang, W. Lee, Nanogap-controlled Pd coating for hydrogen sensitive switches and hydrogen sensors, Sens. Actuators B: Chem. 255 (2018) 1841–1848.
[20] M.M. Hawkeye, M.T. Taschuk, M.J. Brett, Glancing Angle Deposition of Thin Films, (2014), pp. 1–30.
[21] M.M. Hawkeye, M.J. Brett, Glancing angle deposition: fabrication, properties,and applications of micro- and nanostructured thin films, J. Vac. Sci. Technol. A 25 (2007) 1317.
[22] J. Baek, B. Jang, M.H. Kim, W. Kim, J. Kim, H.J. Rim, S. Shin, T. Lee, S. Cho, W. Lee, Sens. Actuators B: Chem. 256 (2018) 465–471.
[23] T.L. Ward, T. Dao, Model of hydrogen permeation behavior in palladium membranes, J. Membr. Sci. 153 (1999) 211–231.
[24] A. Sieverts, W. Danz, Zeitschrift Fur Physikalische Chemie-Abteilung B-Chemie Der Elementarprozesse Aufbau Der Materie 38 (1938), p. 46.
[25] X. Wen, M. Wang, C. Wang, J. Jiang, Electroless plated SnO_2-Pd-Au composite thin film for room temperature H_2 detection, Electrochim. Acta 56 (2011) 6524–6529.
[26] Y. Shen, et al., Microstructure and room-temperature H_2 sensing properties of undoped and impurity-doped SnO_2 nanowires, Chem. Lett. 42 (2013) 492–494.
[27] A.I. Ayesh, S.T. Mahmoud, S.J. Ahmad, Y. Haik, Novel hydrogen gas sensor based on Pd and SnO_2 nanoclusters, Mater. Lett. 128 (2014) 354–357.
[28] I.H. Kadhim, H.A. Hassan, Room temperature hydrogen gas sensor based on nanocrystalline SnO2 thin film using sol-gel spin coating technique, J. Mater. Sci: Mater. Electron. 27 (2016) 4356–4362.
[29] Y. Peng, L. Zheng, K. Zou, C. Li, Enhancing performances of resistivity-type hydrogen sensor based on Pd/SnO2/RGO nanocomposites, Nanotechnology 28 (2017) 215501.
[30] R. Battino, The Ostwald coefficient of gas solubility, Fluid Phase Equilliaria 15 (1984) 231–240.
[31] Standard Test Method for Estimation of Solubility of Gases in Petroleum Liquids, ASTM International D2779-92, 2018D2779-92.
[32] Standard Test Method for Analysis of Gases Dissolved in Electrical Insulating Oil by Gas Chromatography, ASTM International, 2018D3612.
[33] G. Beensh-Marchwicka, L. Krol-Stepniewska, High temperature oxidized SnO_2 films prepared by reactive sputtering, Active Passive Electr. Comp. 12 (1987) 191–200.
[34] I.H. Kadhim, H.A. Hassan, Q.N. Abdullah, Hydrogen gas sensor based on nanocrystalline SnO_2 thin film grown on bare Si substrates, Nano-micro Lett. 8 (2016) 20–28.
[35] S.R. Morrison, Selectivity in semiconductor gas sensors, Sens. Actuators 12 (1987) 425–440.
[36] C. Ling, Q. Xue, Z. Han, H. Lu, F. Xia, Z. Yan, L. Deng, Room temperature hydrogen sensor with ultrahigh-responsive characteristics based on $Pd/SnO_2/SiO_2/Si$ heterojunctions, Sens. Actuators B: Chem. 227 (2016) 438–447.
[37] M.S. Shivaraman, C. Svensson, H. Hammarsten, I. Lundstrom, Hydrogen sensitivity of palladium-thin-oxide-silicon Schottky barriers, Electron. Lett. 12 (1976) 483–484.

Min Hyung Kim was born in 1994 in Seoul, Republic of Korea. She received a BS degree in Material Science and Engineering at Yonsei University in 2017. She is currently studying Hydrogen sensors using various nanostructures as a step toward her MS. Degree at Yonsei University.

Byungjin Jang was born in 1987 in Seoul, Republic of Korea. He received a BS degree in Material Science and Engineering at Yonsei University in 2011. He is currently studying MOTIFE sensors using Pd and gas sensors using various nanostructures as a step toward his pH.D. degree at Yonsei University.

Wonkyung Kim was born in 1976 in Mokpo, Republic of Korea. He received a Ph. D. degree in Material Science and Engineering at Yonsei University in 2018. He has been a adjunct professor of School of Nano & Materials Science and Engineering at Kyungpook National University. In recent years, his research interests have centered on gas sensors.

Wooyoung Lee is a professor of Department of Materials Science and Engineering, the chairman of Yonsei Institute of Convergence Technology and the Head of Institute of Nanoscience and Nanotechnology at Yonsei University in Korea. He received a BS degree in Metallurgical Engineering in 1986, a MS degree in Metallurgical Engineering from the Yonsei University in 1988. He received a Ph.D. degree in Physics from University of Cambridge, England in 2000. He is also the director in Korea-Israel Industrial R&D Foundation and the advisor in National Assembly Research Service. In recent years, his research interests have centered on spintronics, thermoelectric materials and devices, hydrogen sensor, hydrogen gas storage, various gas sensors, rare earth and non-rare earth permanent magnets. He has received a number of awards in nano-related research areas and a Service Merit Medal (2008) from the Korean Governments due to contribution on the development of intellectual properties. He has authored and co-authored over 150 publications, and has edited a few of special books on nano-structured materials and devices.